Thermochimica Acta, 58 (1982) 125–153
Elsevier Scientific Publishing Company, Amsterdam—Printed in The Netherlands

THE ROLE OF TITANIA AND TITANIA MIXTURES IN THE NUCLEATION AND CRYSTALLIZATION OF SPODUMENE–WILLEMITE–DIOPSIDE GLASSES

A.W.A. EL-SHENNAWI, A.A. OMAR

Glass-Ceramic Section, Refractories and Building Materials Laboratory, National Research Centre, Dokki, Cairo (Egypt)

A.M. MORSY

Geology Department, Faculty of Science, Suez Canal University, Ismailia (Egypt)

(Received 20 January 1982)

ABSTRACT

The nucleation and crystallization processes in glasses and melts of different compositions within the system spodumene–willemite–diopside, using different proportions of TiO_2 and mixtures of TiO_2+ZrO_2 and TiO_2+ZrO_2+F as nucleating agents, have been studied by employing a combination of DTA, X-ray diffraction, and optical and scanning electron microscopy. Incorporation of titania or its mixtures in the base composition modified the crystallization kinetics, as expressed by variations observed on the peak temperatures and spans of the DTA exotherms of crystallization. These nucleants also influenced the type and relative proportions of the crystallized phases, transformation temperatures, degree of metastability of β-Zn_2SiO_4 and β-eucryptite ss *, and the texture of the resultant glass-ceramic. TiO_2 additions lowered the onset crystallization temperatures and favoured the crystallizability. TiO_2 catalyzed the pyroxene and β-eucryptite ss formation and also the transformation of the latter into β-spodumene ss. TiO_2+ZrO_2 mixtures enhanced the crystallization but retarded phase transformation. Addition of F to TiO_2+ZrO_2 showed a synergistic effect to the action of TiO_2 and also greatly facilitated willemite formation. The proposed nucleation mechanism of titania and its mixtures involves the enhancement of liquid–liquid phase separation followed by the separation of a zinc titanate phase which heterogeneously nucleates the crystallization of the glass bulk.

INTRODUCTION

'Glass-ceramic' is a generic name given to a material which is first melted, forming a glass, fabricated to shape and then converted through controlled

* ss = solid solution; β-eucryptite ss was also named β-quartz ss in the literature.

0040-6031/82/0000–0000/$02.75

crystallization, by specific heat treatment, into non-porous polycrystalline material. Their texture is characterized by uniform fine-grained randomly oriented crystals with some residual glassy matrix. As a result of this unique microstructure, properties such as translucency, high strength, and very low and uniform thermal expansion can be routinely produced. Glass-ceramic has a number of technical advantages over conventional ceramics. In particular, the wide freedom of choice of composition, raw materials, melting, forming and processing methods and the final properties are to some degree variable so as to suit particular applications [1–3].

The basis for controlled glass crystallization lies in efficient nucleation. Nucleation from the glass surface or from a small number of sites in the interior results in a coarse-grained oriented form of crystallization. This texture is generally accompanied by voids, planes of weakness, gross distortion of the material and consequently results in low strength [4]. The discovery of the role of nucleating agents [5,6] in initiating glass crystallization from a multitude of centres was the most effective factor in glass-ceramic production. Without this nucleating catalyst bulk fine crystallization does not generally occur. Changing the nucleating agent, its concentration and/or mixing it with others greatly changes the appearance, the crystalline phases and the crystallite size in the resultant glass-ceramic [7]. Of the many nucleating agents studied, especially in lithia aluminosilicates and related compositions, TiO_2 [5–13], ZrO_2 [14–18], and mixtures of TiO_2 and ZrO_2 [17–23] appear to be the most commonly used.

The present work is primarily concerned with the study of the crystallization of different mixtures within the system, spodumene($LiAlSi_2O_6$)–willemite (Zn_2SiO_4)–diopside($CaMgSi_2O_6$), whose end members represent the most promising glass-ceramic-forming phases. Dealings relating these end members to each other are sparse and very scarce. The main object of this paper is to study the effect of different concentrations of TiO_2, and mixtures of $TiO_2 + ZrO_2$ and $TiO_2 + ZrO_2 + F$ on the crystallization from both the glass and molten states using DTA, X-ray diffraction, and optical and electron microscopy. By coupling X-ray diffraction with electron microscopic examination the nucleation process and sequence of crystallization were more elucidated.

EXPERIMENTAL

Compositions and glass preparation

The glass compositions chosen in this study are defined by Fig. 1 and Table 1. Most of the work reported here concerns glass composition no. 9

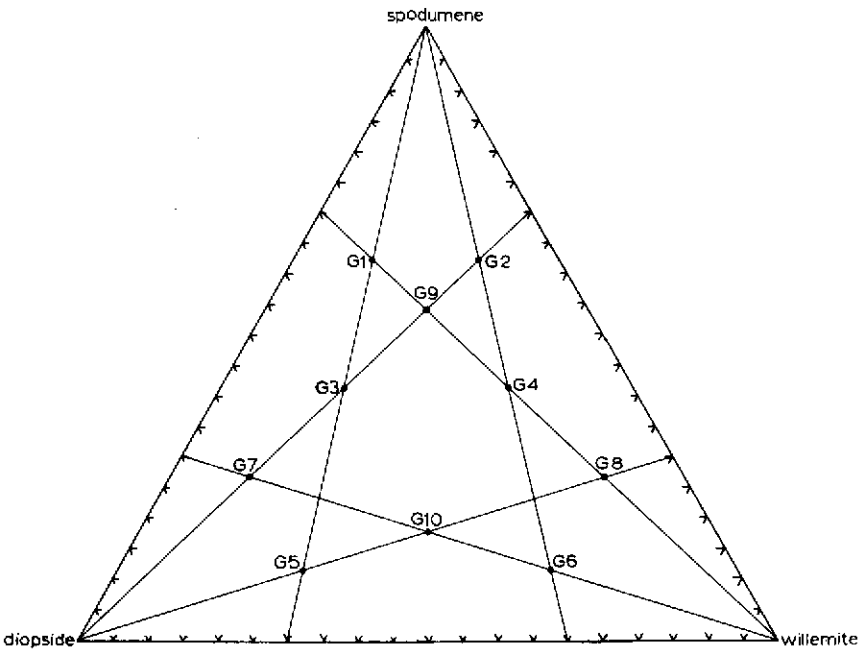

Fig. 1. Ternary mole % diagram of the spodumene–willemite–diopside system showing the compositions studied.

TABLE 1

Composition of the investigated base glasses

No.	Constituent compounds (mole %)			Constituent oxides (wt. %)					
	Spodumene	Willemite	Diopside	Li_2O	CaO	MgO	ZnO	Al_2O_3	SiO_2
G1	62.0	11.4	26.6	4.98	6.89	4.95	8.33	16.98	57.87
G2	62.0	26.6	11.4	4.98	2.95	2.12	19.43	16.98	53.54
G9	54.0	23.0	23.0	4.34	5.96	4.28	16.80	14.79	53.83
G3	41.2	17.6	41.2	3.31	10.67	7.67	12.85	11.29	54.21
G4	41.2	41.2	17.6	3.31	4.56	3.27	30.09	11.29	47.48
G7	26.6	11.4	62.0	2.13	16.06	11.54	8.33	7.29	54.65
G8	26.6	62.0	11.4	2.13	2.95	2.12	45.28	7.29	40.23
G10	17.6	41.2	41.2	1.41	10.67	7.67	30.09	4.82	45.34
G5	11.4	26.6	62.0	0.92	16.06	11.54	19.43	3.12	48.93
G6	11.4	62.0	26.6	0.92	6.89	4.95	45.28	3.12	38.84

(G9), which is almost representative of the high-spodumene glasses (viz. G1, G2, G9, G3 and G4).

The glasses were prepared from high purity Li_2CO_3, $CaCO_3$, $MgCO_3$, ZnO, Al_2O_3, SiO_2, TiO_2, ZrO_2 and CaF_2. The calculated proportions were thoroughly mixed and melted in fireclay Morganite crucibles in a gas-fired furnace, at about 1450°C for 2.5–3.5 h, depending on the glass composition. The homogeneity of the melt was achieved through the swirling of the melt-containing crucible several times at about 20 min intervals, and was checked in the resulting glass by the petrographic microscope. Specimens for heat-treatments were prepared in the form of buttons. To keep thermal history effects to a minimum, the specimens were not annealed and air cooled.

0.0, 2.5, 5.0 and 7.5% TiO_2 and combinations of each of these with 0.2 and 0.4% ZrO_2 (% by wt. above 100%) as well as a mixture of 5.0% TiO_2 + 0.4% ZrO_2 + 1.0% F were investigated. For simple reference to the nucleation agent content, the following abbreviation is used throughout this work. The glass number, for example no. 9 (G9), is followed by a term which represents the weight percentages of TiO_2, ZrO_2, and F; for example G9-5t + 0.4z + 1f.

Heat-treatments

A slow gradual cooling regime from the melt, and single- and double-stage heat-treatment schedules were adopted to induce crystallization in the melts and glasses: (i) The slow gradual cooling regime; in which the melt was cooled in an electric furnace at a rate of 10°C h^{-1} starting from 1400 down to 600°C, after which the furnace was switched off and the sample cooled inside it to ambient temperature. The whole process usually took about 92 h. (ii) For single stage heat-treatment; glass buttons were reheated in a muffle furnace to the required temperature in the 720–1000°C temperature range (in accordance with the DTA results) at 30 or 60°C intervals for 1, 2, 3, 5, or 15 h and then air-quenched. (iii) In double-stage heat-treatment; the specimens were heated to a certain temperature in the 150°C-precrystallization temperature range for 4 h (in some cases from 0 up to 24 h at 2 h intervals followed by rapid cooling) after which the process was repeated at a higher temperature. Temperatures were measured using a standardized Pt–Pt 10% Rh thermocouple placed alongside the specimen.

Further details of the actual heat-treatment cycles concerned are given with each of the glasses studied.

X-Ray diffraction analysis

Powder X-ray diffraction patterns were obtained using a Phillips X-ray diffractometer type PW 1050, adopting Ni-filtered Cu radiation for some of

the samples and Fe-filtered Co radiation for some others, operated at 36 kV and 16 mA, and 28 kV and 10 mA, respectively. The scanning rate 1° 2θ min^{-1}. All the instrument settings were maintained for all the analyses and an external standard, namely a Si disc, was always used to test this maintenance. Errors due to filling of sample holders were also avoided. This was necessary to make the comparative phase frequency based on the peak height more accurate.

Differential thermal analysis

A Hungarian-made MOM derivatograph, model OD-102, was used. One of the cups was filled with the −200 mesh glass sample, the other with alumina as a standard inert material. The two cups were inserted into the tube furnace which was heated from ambient temperature up to 1000°C at a rate of 10°C min^{-1}. Two graphs were drawn on the chart, one for the calculation of the exact temperature and the other was the DTA curve.

Scanning electron microscopy

The broken fragments of the as-cast and heat-treated glasses were coated with a thin film of gold. The specimens were placed in a Nanolab-7 scanning electron microscope (Semco, Canada) which had separate display channels for visual observation and photographic recording. Representative scanning electron micrographs were selected from several made of each specimen as a result of much visual observation and selection of each area of the glass surface.

Petrography

The mineralogical constitution as well as textures of heat-treated samples were optically examined in thin sections using a polarizing Carl Zeiss research microscope.

RESULTS

Crystallization behaviour

Single-stage heat-treatment

Study of the crystallization behaviour, over the temperature range investigated in this work, revealed that β-eucryptite ss and/or β-spodumene ss, pyroxene, β-Zn_2SiO_4 and/or willemite were the main crystalline phases

TABLE 2

Phases developed in some glasses nucleated by titania and titania mixtures

Glass number	Heat treatment	Phases developed
G9	900, 3 h	β-Eucryptite, willemite, diopside, β-Zn silicate (tr)
G9-2.5t	900, 3 h	β-Eucryptite, willemite, titanaugite
	1000, 3 h	β-Spodumene, willemite, titanaugite
G9-2.5t+0.4z	900, 3 h	β-Eucryptite, titanaugite, willemite
	1000, 3 h	β-Spodumene, titanaugite, willemite
G9-5t	750, 3 h	β-Eucryptite, titanaugite
	900, 3 h	β-Spodumene, β-eucryptite, titanaugite, willemite
	1000, 3 h	β-Spodumene, titanaugite, willemite
G9-5t+0.2z	900, 3 h	β-Eucryptite, β-spodumene, titanaugite, willemite
	1000, 3 h	β-Spodumene, willemite, titanaugite, β-eucryptite (tr ?)
	Slow cooling	Siliceous-β-spodumene, gahnite, diopside, Zn-titanate (m)
G9	Slow cooling	β-Spodumene, willemite, diopside, gahnite (tr?)
G9-5t+0.4z	660, 5 h	Amorphous
	690, 5 h	β-Eucryptite (tr), Zn-titanate (tr?)
	720, 5 h	β-Eucryptite, titanaugite, Zn-titanate (tr?)
	750, 3 h	β-Eucryptite, titanaugite
	900, 3 h	β-Eucryptite, titanaugite, willemite, β-spodumene (m)
	1000, 3 h	β-Spodumene, titanaugite, willemite, β-eucryptite (tr)
	1000, 5 or 15 h	β-Spodumene, titanaugite, willemite
G9-5t+0.4z+1f	750, 3 h	β-Eucryptite, willemite, diopside (m), fluorite (tr)
	900, 3 h	β-Spodumene, willemite, pyroxene, β-eucryptite (tr), fluorite (tr)
	1000, 3 h	β-Spodumene, willemite, pyroxene, fluorite
G9-7.5t	750, 3 h	β-Eucryptite, titanaugite, Zn-titanate (tr?)
	900, 3 h	β-Spodumene, β-eucryptite, titanaugite, willemite, Zn-titanate
	1000, 3 h	β-Spodumene, titanaugite, willemite, Zn-titanate
G9-7.5t+0.4z	690, 5 h	β-Eucryptite (m), titanaugite (tr), Zn-titanate (tr)

TABLE 2 (continued)

Glass number	Heat treatment	Phases developed
	750, 3 h	β-Eucryptite (siliceous), titanaugite, Zn-titanate (m)
	900, 3 h	Siliceous-β-spodumene, β-eucryptite, titanaugite, Zn-titanate
	1000, 3 h	Siliceous-β-spodumene, titanaugite, Zn-titanate (m), β-eucryptite (m)
	1000, 5 h	Siliceous-β-spodumene, titanaugite, Zn-titanate
G1	750, 3 h+780, 3 h	β-Eucryptite, diopside (m)
G1-5t	750, 3 h	β-Eucryptite, titanaugite
G1-5t+0.4z	750, 3 h	β-Eucryptite, titanaugite
G1	900, 3 h	β-Eucryptite, diopside, willemite
G1-2.5t	900, 3 h	β-Eucryptite, pyroxene, willemite, β-spodumene
G1-5t	900, 3 h	β-Spodumene, titanaugite
G1-5t+0.4z	900, 3 h	β-Spodumene, titanaugite, β-eucryptite (m)
G2	750, 3 h+780, 3 h	β-Eucryptite, β-Zn_2SiO_4
G2-5t	750, 3 h	β-Eucryptite, willemite, titanaugite (m), β-Zn_2SiO_4(tr)
G2-5t+0.4z	750, 3 h	β-Eucryptite, willemite, titanaugite, β-Zn_2SiO_4 (tr ?)
G2	900, 3 h	β-Eucryptite, willemite, β-Spodumene (tr)
G2-5t	900, 3 h	β-Eucryptite, willemite, β-spodumene (m), titanaugite (m)
G2-5t+0.4z	900, 3 h	β-Eucryptite, willemite, titanaugite, β-spodumene (tr)
G3	900, 3 h	β-Eucryptite, diopside, willemite
G3-5t	900, 3 h	β-Eucryptite, titanaugite, willemite
G4	750, 3 h+780, 3 h	β-Eucryptite, β-Zn_2SiO_4
G4-5t	750, 3 h	β-Eucryptite, willemite, titanaugite
G4-5t+0.4z	750, 3 h	β-Eucryptite, willemite, titanaugite
G4	900, 3 h	β-Spodumene, willemite, β-eucryptite
G4-5t	900, 3 h	β-Eucryptite, willemite, β-spodumene, titanaugite
G4-5t+0.4z	900, 3 h	β-Eucryptite, willemite, titanaugite
G4-2.5t	1000, 3 h	β-Spodumene, willemite, titanaugite
G8	750, 3 h+780, 3 h	Willemite, β-Zn_2SiO_4, β-eucryptite
G8-5t	750, 3 h	Willemite, siliceous-β-eucryptite, titanaugite (m)
G8	900, 3 h	Willemite, β-eucryptite, β-spodumene
G8-2.5t	900, 3 h	Willemite, β-spodumene, β-eucryptite, titanaugite (tr)
G8-5t	900, 3 h	Willemite, siliceous-β-spodumene, β-eucryptite, titanaugite (m)

TABLE 2 (continued)

Glass number	Heat treatment	Phases developed
G6	900, 3 h	Weak crystallization
G6-5t	900, 3 h	Willemite, titanaugite (m), cristobalite (tr ?)

Phases arranged in a decreasing order.
m = minor, tr = traces, ? = uncertain.

developed in almost all nucleated and non-nucleated glasses (Table 2). In general, most of the nucleant-free glasses (e.g., G1, G4, G9 and G8) began to crystallize at about 780°C, while glasses with TiO_2 or $TiO_2 + ZrO_2$ began at about 750°C, and with additional F at about 720°C.

On heating for 3 h at 750°C, solid solutions of both β-eucryptite and pyroxene types and traces of β-Zn_2SiO_4 phase were crystallized out from these nucleated glasses (except G9-5t + 0.4z + 1f where fair amounts of willemite were detected in these early stages of crystallization). In the absence of these additives (in G9), β-eucryptite ss, β-Zn_2SiO_4 and minor diopside were obtained in the fully crystallized sample under almost analogous conditions. With increase in temperature, the β-Zn_2SiO_4 transforms into its stable alpha-form, willemite, (around 840°C in G9). At still higher temperatures, the β-eucryptite ss begins to transform into β-spodumene ss.

However, willemite did not develop in G9-7.5t + 0.4z and was detected in relatively lesser amounts in G9-7.5t. Titanaugite, β-spodumene ss, and traces of β-eucryptite ss were the main crystalline phases developed in G9-7.5t + 0.4z at 900 and 1000°C. A minor crystalline phase developed in cases of the disappearance of willemite, in G9-7.5t + 0.4z and G9-7.5t, was identified by X-ray diffraction as Zn_2TiO_4 ss. Associated with the development of this phase the main diffraction peaks of the β-spodumene ss were always displaced to higher 2θ values (e.g., $d = 3.44$ Å; Figs. 2 and 3) in comparison with those developed from other glasses. On the other hand, while the relative line intensities of β-spodumene ss in G9-7.5t + 0.4z were relatively decreased, the intensity of the 2.53 Å diffraction line (corresponding to pyroxene ss, titanaugite, and Zn_2TiO_4 ss phases) was considerably increased. (The crystallized titanaugites are optically non-pleochroic in thin sections, in contrast to distinct pleochroism observed in natural titanaugites [24]. This was attributed to the presence of Ti^{4+}, instead of Ti^{3+}, in synthetic titan-pyroxene formed in air and also to the absence of Fe^{2+} and Fe^{3+} ions [25].)

It was observed that TiO_2 has a catalytic effect on the transformation of

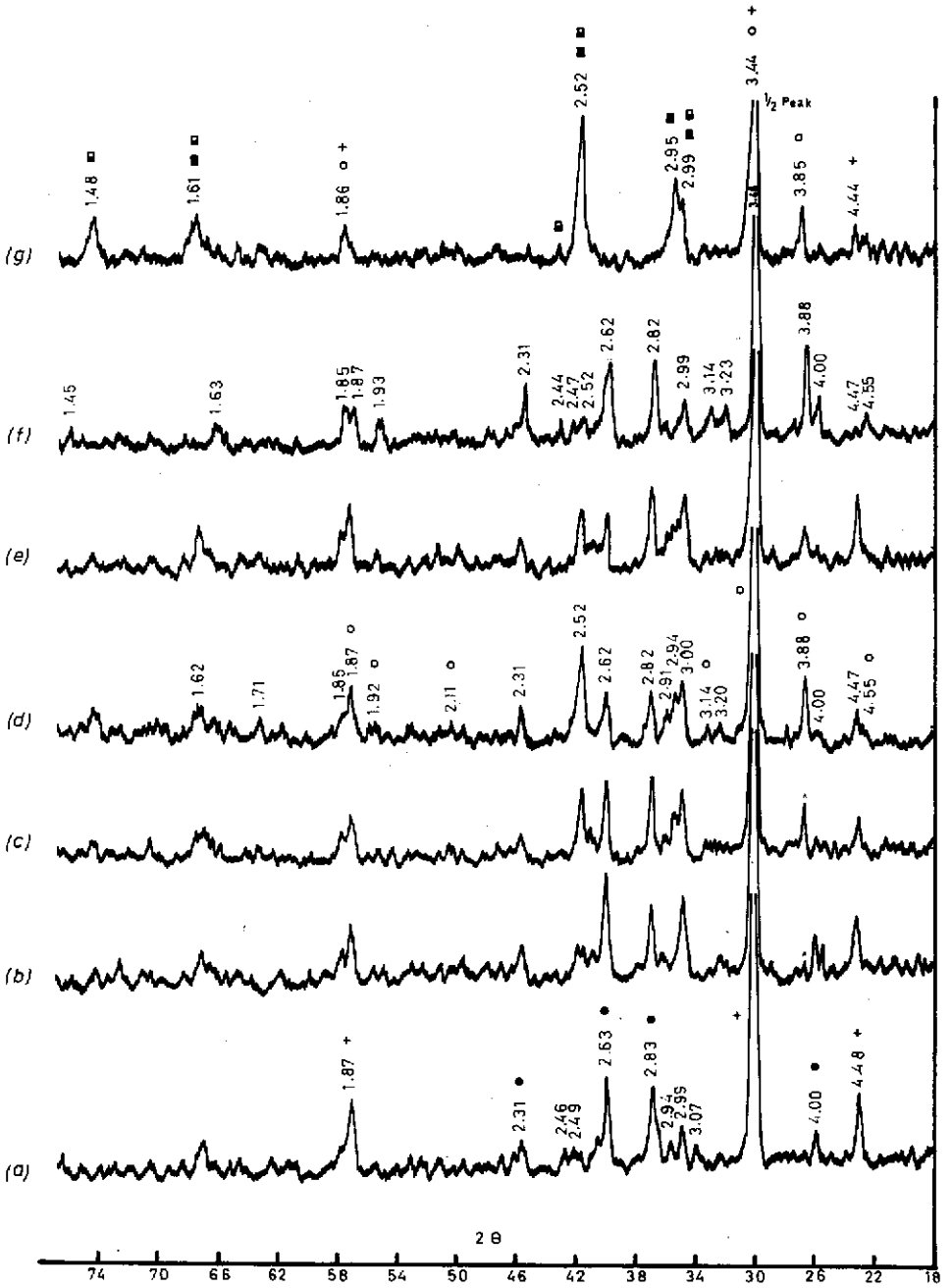

Fig. 2. X-Ray diffraction patterns of glasses no. 9 crystallized at 900°C for 3 h (a) without additives, (b) with 2.5% TiO_2, (c) with 5.0% TiO_2, (d) with 7.5% TiO_2, (e) with 5.0% TiO_2 + 0.4% ZrO_2, (f) with 5.0% TiO_2 + 0.4% ZrO_2 + 1.0% F, and (g) with 7.5% TiO_2 + 0.4% ZrO_2. ○, β-Spodumene ss; +, β-ecuryptite ss; ■, titanaugite; ●, willemite; ◒, Zn titanate ss. CoK_α.

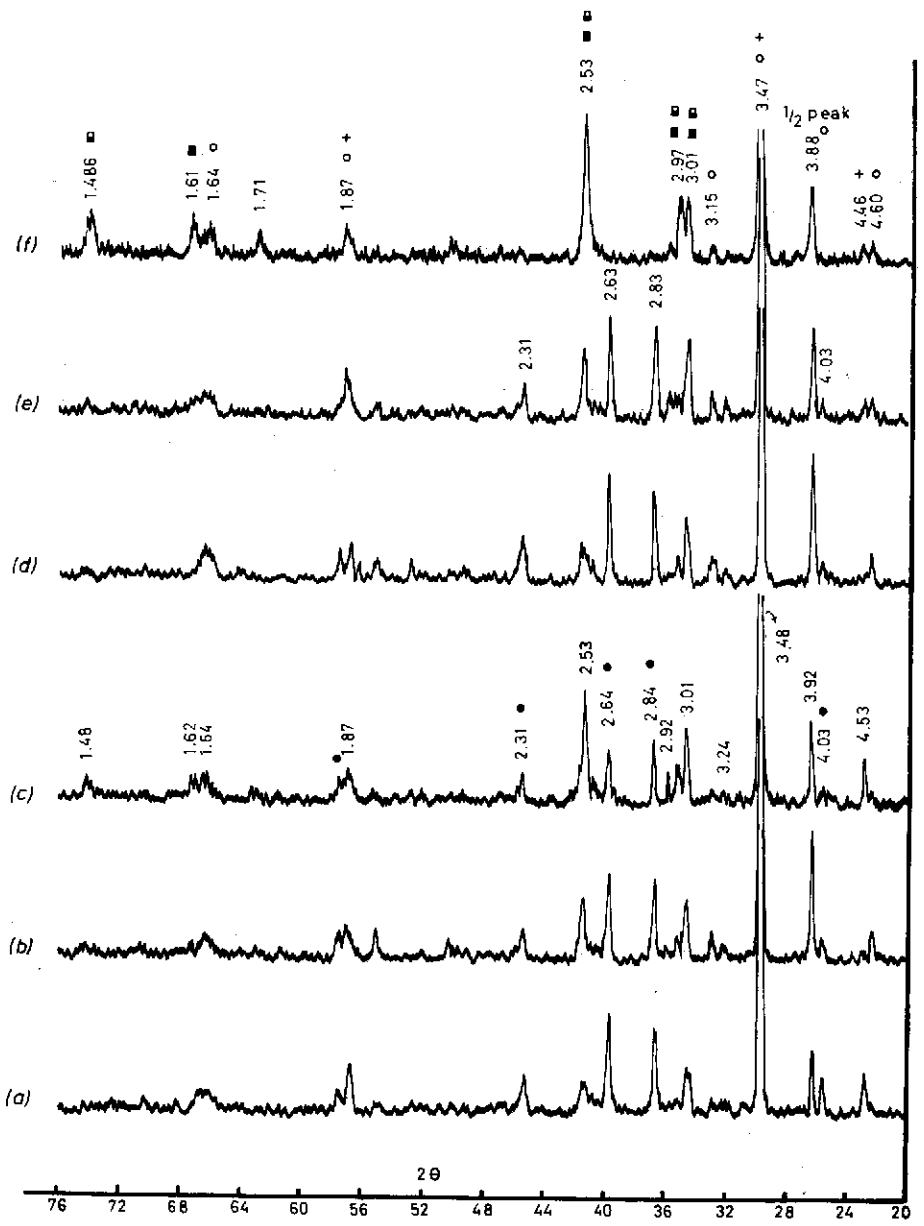

Fig. 3. X-Ray diffraction patterns of glasses no. 9 crystallized at 1000°C for 3 h; (a) with 2.5% TiO_2, (b) with 5.0% TiO_2, (c) with 7.5% TiO_2, (d) with 2.5% TiO_2 + 0.4% ZrO_2, (e) with 5.0% TiO_2 + 0.4% ZrO_2, and (f) with 7.5% TiO_2 + 0.4% ZrO_2. ○, β-Spodumene ss; ■, titanaugite; ●, willemite, +, β-eucryptite ss; ▬, Zn titanate ss. CoK_α.

β-eucryptite ss into β-spodumene ss which increased as the concentration of TiO_2 increased (a progressive increase in the diagnostic 3.88 Å of β-spodumene was observed as the titania content was inceased from 0.0% to 7.5%; patterns (a)–(d) Fig. 2). Addition of 0.4% ZrO_2 to TiO_2 widens the stability field of the metastable β-eucryptite ss; i.e., shifts the transformation temperatures to higher values. For example, the lithia-bearing minerals, crystallized at 900°C in G9-5t + 0.4z, were β-eucryptite ss (refer to 4.47 Å peak) and minor β-spodumene ss while sample G9-5t, with titania only, contained

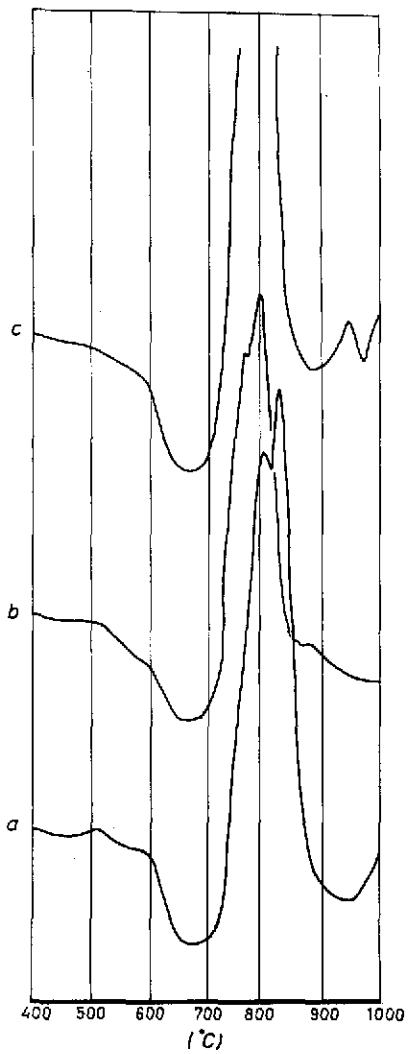

Fig. 4. DTA curves of glass no. 9; (a) with 5.0% TiO_2 + 0.4% ZrO_2, (b) with 5.0% TiO_2 + 0.4% ZrO_2 + 1.0% F, and (c) with 5.0% TiO_2.

more β-spodumene ss rather than β-eucryptite ss [cf. pattern (è) with (c) in Fig. 2]. This may also be noticed on the DTA curves where the exothermic peak corresponding to this transformation occurred at about 970°C [Fig. 4(c)] while it was displaced to higher temperatures, around 1000°C, when 0.4% ZrO_2 was admixed by 5% TiO_2 [Fig. 4(a)].

The addition of 1.0% F to 5% TiO_2 + 0.4% ZrO_2 nucleation mixture dramatically reduced the temperature at which the β-spodumene ss starts to appear and that at which the β-eucryptite ss finally disappears. The lithia-minerals developed in G9-5t + 0.4z + 1f at 900°C were mainly β-spodumene ss and traces of β-eucryptite ss [Fig. 2(f)] whereas those in G9-5t + 0.4z were essentially β-eucryptite ss and minor β-spodumene ss [Fig. 2(e)]. The addition of F also lowered the onset of the crystallization temperature. This can be noticed by comparison of their DTA curves; Figs. 4(a) and (b). The major exothermic crystallization peaks at about 770°C in G9-5t + 0.4z + 1f and at 810°C in G9-5t + 0.4z are mainly due to the formation of β-eucryptite ss, and those at 890 and above 1000°C, respectively, are due to its transformation into β-spodumene ss. Therefore, the temperature at which β-eucryptite ss forms is lowered by about 40°C, and that of its conversion into β-spodumene ss is lowered by about 130°C when 1% F was admixed with the 5% TiO_2 + 0.4% ZrO_2-nucleation mixture. It is also worth mentioning that these mixed nucleants greatly facilitate willemite formation even at the earliest stages of crystallization. The X-ray analysis of the material treated at 900°C revealed fair amounts of willemite, minor pyroxene and fluorite besides the major lithia minerals. This pyroxene is probably slightly subcalcic, since

Fig. 5. Photomicrograph of G9-2.5% TiO_2; 780°C/2 h. Minute star-like skeletals and radial fibrillar growths of β-eucryptite ss and pyroxene exhibiting heterogeneous coarse-grained texture. Crossed nicols, ×62.

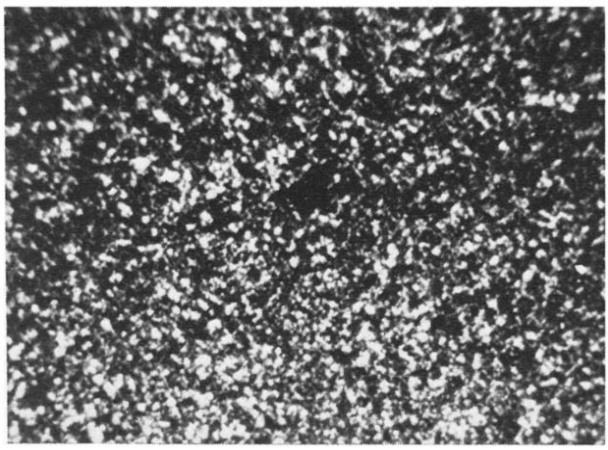

Fig. 6. Photomicrograph of G9-7.5% TiO_2; 780°C/2 h. Fine-grained, nearly holocrystalline mass of β-eucryptite ss and titanaugite. Crossed nicols, ×150.

there is considerable fluorite formation in the investigated glasses [$d = 3.14$ and 1.93 Å, Fig. 2(f)].

As regards textures, microscopic examination of the nucleated glasses (subjected to single-stage treatments for 2 or 3 h in the 720–1000°C range) showed that glasses nucleated with 2.5% TiO_2 or 2.5% TiO_2 + 0.4% ZrO_2 produced crystalline materials with non-uniform coarse-grained textures implying the lowest nucleation density (e.g., Fig. 5). Additions of more than 2.5% TiO_2 led to volume crystallization at low temperatures, up to 810°C. The materials obtained were almost holocrystalline with uniform relatively

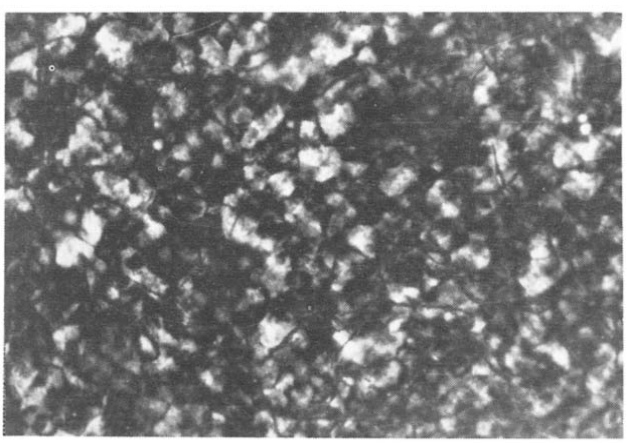

Fig. 7. Photomicrograph of G9-5% TiO_2 + 0.4% ZrO_2 + 1% F; 780°C/2 h. Relatively fine-grained holocrystalline mass of irregularly shaped intergrowths of β-eucryptite ss and titanaugite. Crossed nicols, ×250.

fine-grained textures (e.g. Figs. 6 and 7). This also indicates that the high crystallization rate observed upon introduction of 5 or 7.5% TiO_2 or their mixtures is mainly due to an increased nucleation rate. However, an increase in temperature or time produced a slightly coarser texture with different degrees of development. The double stage treatments (mentioned below) further emphasized that the formation of fine-grained textures is dependent on the concentration of titania or titania nucleation mixtures.

Slow cooling heat-treatment

Crystallization of G9-5t + 0.2z directly from the melt through the slow gradual cooling regime, gave nearly holocrystalline material of siliceous β-spodumene ss, gahnite, diopside, rutile, and Zn_2TiO_4 phase. Attention should be drawn to this material, where willemite or any other zinc silicate phase was developed. In this respect, it is quite different from either its nucleant-free analogue or that resulting from treatment of the corresponding glasses [Fig. 8(a)–(d)]. Moreover, the β-spodumene ss was directly crystal-

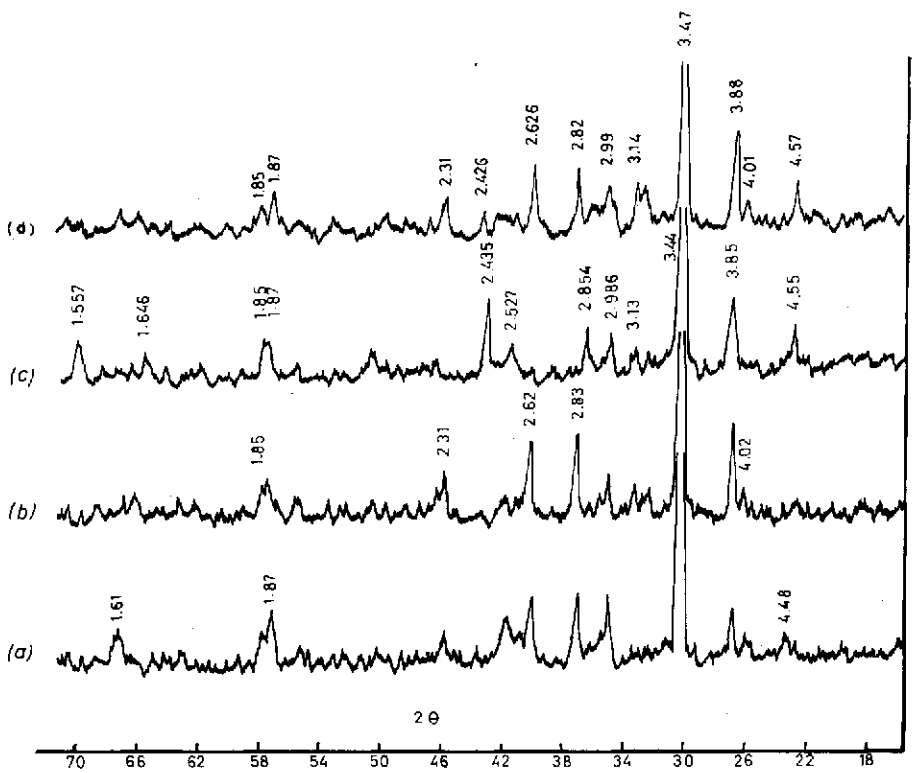

Fig. 8. X-Ray diffraction patterns of glass no. 9 with 5.0% TiO_2 + 0.2% ZrO_2 crystallized at 900°C for 3 h. (a), at 1000°C for 3 h (b), and through the slow gradual cooling regime (c), and G9 (without nucleants) through slow gradual cooling regime (d). CoK_α.

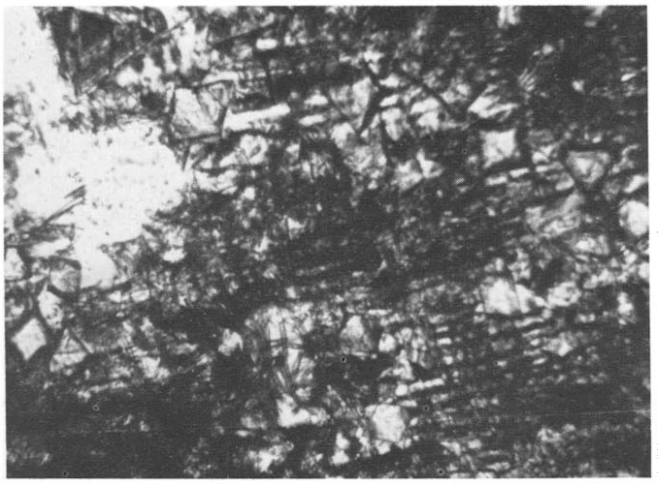

Fig. 9. Photomicrograph of G9-5.0% TiO_2 +0.2% ZrO_2; slow cooling regime. Growths of β-spodumene ss crystals with fine gahnite octahedrons, diopside microlites, and needles of rutile. Crossed nicols, ×250.

lized from the melt with no intermediate β-eucryptite ss stage.

Microscopically, the material consisted of anhedral to subhedral β-spodumene ss crystallites, a fair amount of fine gahnite octahedrons, some diopsidic microlites and minor minute needles of rutile. All these are embedded in a felted irregular cryptocrystalline groundmass. At high magnification, this groundmass was found to be stippled by tiny cubes and oc-

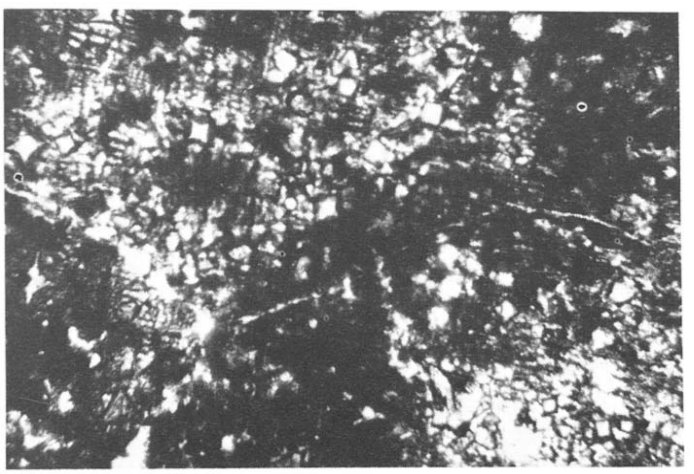

Fig. 10. Photomicrograph of G9-5.0% TiO_2 +0.2% ZrO_2; slow cooling regime. Minute anhedral β-spodumene ss crystallites, gahnite octahedrons, diopside microlites, and needles of rutile in a felted cryptocrystalline groundmass. Crossed nicols, ×150.

tahedrons (with extreme relief) of Zn_2TiO_4 phase (Figs. 9 and 10).

X-Ray diffraction revealed only silica-rich β-spodumene ss, gahnite and diopside. The other phases were not certainly verified due to their minor amounts. The β-spodumene ss, developed under conditions of slow cooling, was more siliceous than in the nucleant-free analogue [e.g. the main diffraction line was displaced to 3.444 Å, Fig. 8(c) and (d)]. The formation of gahnite in this sample (instead of willemite as in nucleant-free or in heat treated G9-5t + 0.2z glasses) resulted in the formation of β-spodumene solid solutions with higher silica or lower alumina contents.

Nucleation effects

The nucleation effects were studied, in thin sections, on almost all the nucleated glasses; which were heated for 4 h in 600–690°C range at 30°C intervals followed by growth treatment at 720 or 750°C for 15 or 30 min. More detailed investigation on the nucleation mechanism and the sequence of crystallization of G9-5t + 0.4z and G9-7.5t + 0.4z is afforded by scanning electron microscopy and X-ray diffraction analysis. In the latter case, the samples were heat treated for 4 h in the nucleation stage and the effect of nucleation time (from 0 up to 24 h at 2 h intervals) was also studied at their optimum nucleation temperature (660°C). The effect of optimum nucleation temperatures and time on the crystallization temperatures for only 1 h was also studied.

The colours of these nucleated-glasses treated only in the nucleation stage were changed from yellow-amber in the untreated glasses to a bluish violet

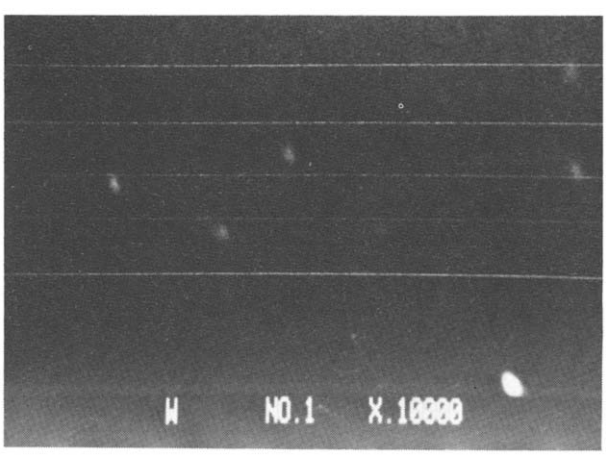

Fig. 11. Scanning electron micrograph of G9-7.5% TiO_2 +0.4% ZrO_2; as-cast. Clear homogeneous glass.

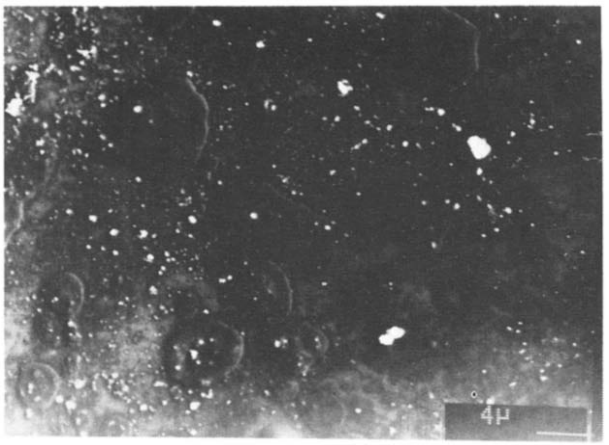

Fig. 12. Scanning electron micrograph of G9-7.5% TiO_2 + 0.4% ZrO_2; 600°C/4 h. Spherical elevations and circular patches indicating gross phase separation.

after nucleation treatment. More insight into the nature of these changes in visual appearance is also delineated by electron microscopy and spectrophotometry and will be discussed elsewhere.

The untreated glass (as-cast) appears homogeneous before reheating and the scanning electron microscopy gave no evidence of phase separation (Fig. 11). After 4 h treatment at 600°C, the scanning electron micrograph of a fresh fractured surface of the sample, shown in Fig. 12, revealed spherical elevations (spheroidal aggregates) and circular patches, which appear to have a smoother surface than the matrix, implying a macroscopic amorphous phase separation. As the heat treatment progressed to 660°C as well as for

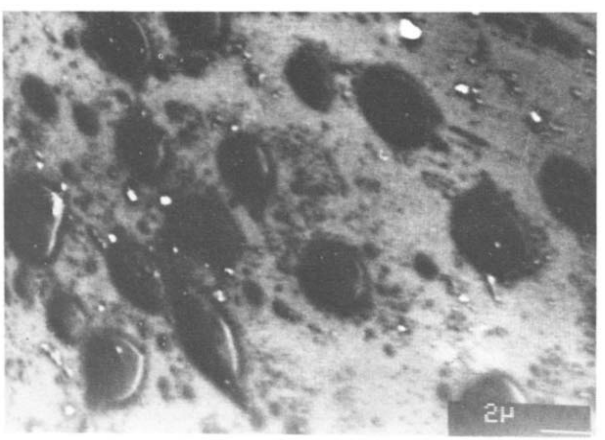

Fig. 13. Scanning electron micrograph of G9-7.5% TiO_2 + 0.4% ZrO_2; 660°C/8 h. Similar spheroidal aggregates exhibiting amorphous phase separation.

longer periods up to 10 h, nearly similar spheroidal aggregates were observed but with little changes in the overall number and size (e.g. Fig. 13). When the samples of 660°C treatments were X-rayed, they gave diffraction patterns with diffuse maxima in the region of the most intense β-eucryptite ss diffraction peaks. This indicates that although β-eucryptite is not yet crystallized, a considerable ordering of the glass structure has occurred with the formation of short-range regions structurally similar to β-eucryptite ss. Specimens with prolonged heat treatments for 12 up to 24 h at 660°C were almost similar to those treated at slightly higher temperatures, e.g. at 690°C for 4 h. All showed incipient crystallization. The micrographs (Figs. 14–16) showed minor polygonal structures, hexagons and biconical growths. At high magnification and by careful inspection, tiny diffused crystalline patches, which are presumably the original β-eucryptite nuclei, were just observed almost at the center of some hexagons. The X-ray diffraction of 690°C treatments show positive very weak diffraction patterns with *d* spacings at 3.45, 2.90, 2.56–2.43 and 1.47 Å. These lines are due to a β-eucryptite phase although the existance of a zinc titanate phase ss cannot be excluded. However, Zn_2TiO_4 possesses *d* spacings at 2.55 (100), 1.62 (90), 1.47 (100) and 2.99 (40) [26]. These diffraction peaks were somewhat difficult to follow since they were superimposed on the diffraction lines of titanaugite which was immediately (or simultaneously) formed after the β-eucryptite ss. The crystallinity increased sharply over a narrow temperature range so that at 720°C G9-5t + 0.4z had crystallized mainly into β-eucryptite ss and diopside ss and G9-7.5t + 0.4z into β-eucryptite ss, titanaugite and traces of Zn_2TiO_4 ss. This indicates that the last phase was more dinstinct in higher titania concentrations.

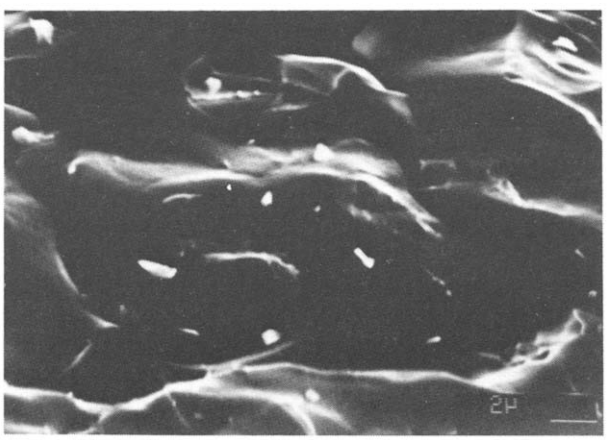

Fig. 14. Scanning electron micrograph of G9-7.5% TiO_2 + 0.4 ZrO_2; 660°C/12 h. Structureless glass showing incipient crystallization.

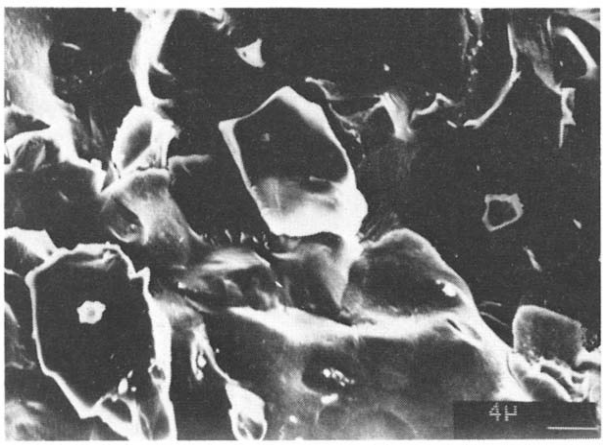

Fig. 15. Scanning electron micrograph of G9-7.5% TiO_2 +0.4% ZrO_2; 660°/24 h. Polygonal structures, hexagons and biconical growths of β-eucryptite ss in glassy matrix.

Although numerous heat-treatments were applied for nucleation and crystallization, no quantitative measurement of either nucleation or crystallization rates was possible. This is because the crystallization of most of the nucleated glasses was too rapid to permit convenient observation. However, nucleation treatment of G9-5t + 0.4z, G9-7.5t and G9-7.5t + 0.4z at 600°C resulted in minimum nucleations, whereas treatment at 630°C led to a formation of a large number of hedritic or biconical crystallites (Fig. 17). As the nucleation temperature was increased to 660°C, the nucleation density was much higher and the crystallites occupied almost the entire volume of

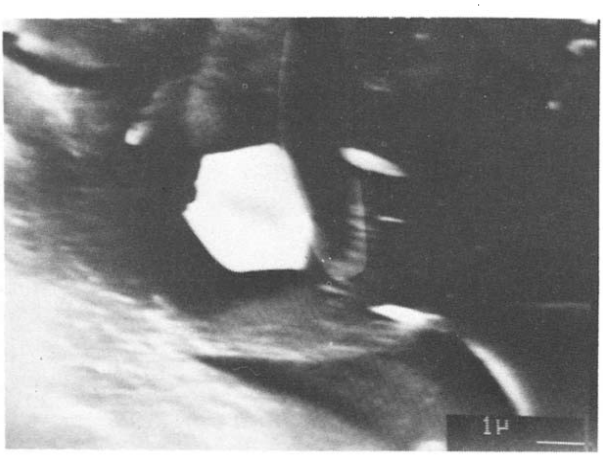

Fig. 16. Scanning electron micrograph of G9-7.5% TiO_2 +0.4% ZrO_2; 690°C/4 h. Hexagon of β-eucryptite ss in glassy base.

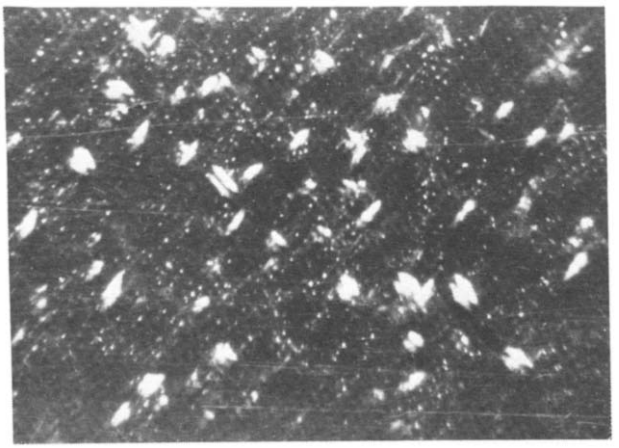

Fig. 17. Photomicrograph of G9-5.0% TiO_2 + 0.4% ZrO_2; 630°C/4 h + 750°C/1/2 h. Some hedritic and biconical β-eucryptite ss crystallites in glassy base. Crossed nicols, × 150.

the sample (Fig. 18). The nucleation density attained its maximum around this temperature, since a further rise in temperature to 690°C had a slight relative coarsening effect. On the other hand, it was found that a nucleation treatment time greater than 4 h had very little effect on the nucleation density, and the microstructures were almost similar even for a 16 h treatment (Fig. 19). A similar trend was also observed in G9-5t, G9-5t + 0.2z and G9-5t + 0.4z + 1f, but with a slight displacement of the whole nucleation picture to lower temperatures (by about 30°C). The maximum nucleation

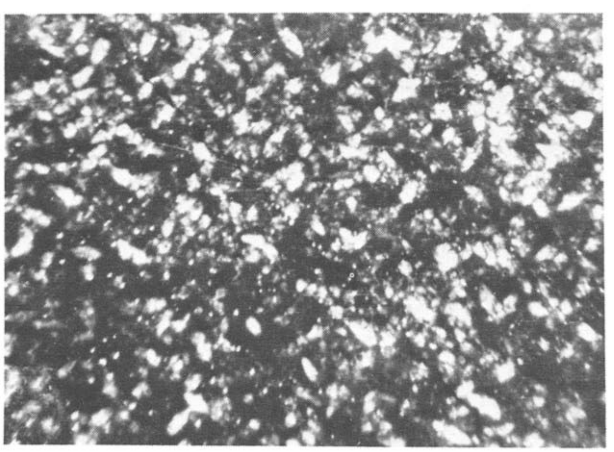

Fig. 18. Photomicrograph of G9-5.0% TiO_2 + 0.4% ZrO_2; 660°C/4 h + 750°C/1/2 h. The β-eucryptite ss growths exceedingly increased indicating a maximum nucleation density. Crossed nicols, × 150.

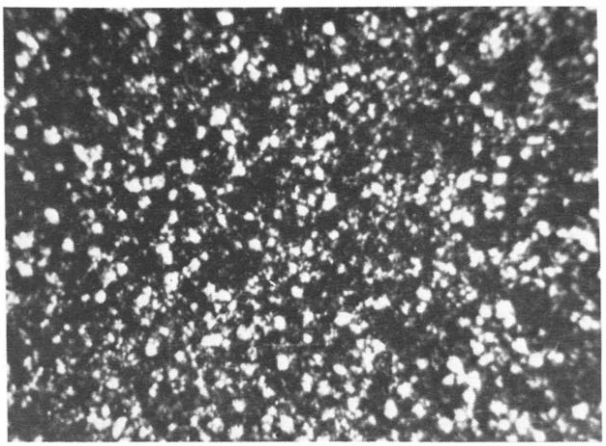

Fig. 19. Photomicrograph of G9-5.0% TiO_2 +0.4% ZrO_2; 660°C/16 h+750°C/1/2 h. Nearly similar to Fig. 18; the growths occupied almost the entire bulk. Crossed nicols, ×150.

densities appeared around 630°C after 4 h treatment.

When specimens of the above mentioned nucleated glasses were two-step heat treated (for 4 h at their optimum nucleation temperatures, 630–660°C, and then for 1 h only at 750, 780, 810, 900, or 1000°C), almost holocrystalline glass-ceramics with fine-grained uniform textures were produced (Figs. 20–25). The finer textures were always observed in samples given the lower crystallization temperature treatment (cf., Fig. 24 with Fig. 25) as well as in those containing the highest nucleant contents (cf., Fig. 23 with Fig. 20).

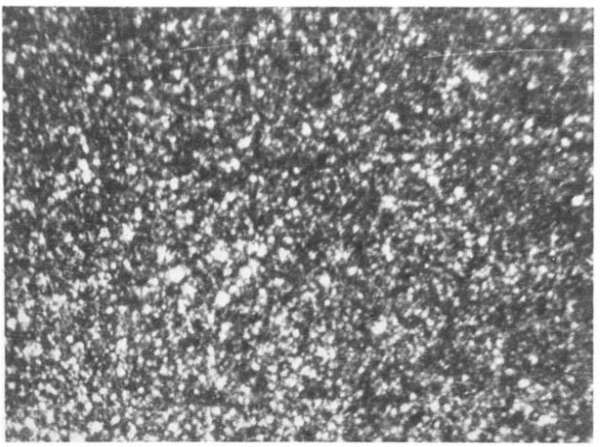

Fig. 20. Photomicrograph of G9-5.0% TiO_2; 630°C/4 h + 780°C/1 h. Holocrystalline mass of β-eucryptite ss, titanaugite and willemite exhibiting a fine-grained texture. Crossed nicols, ×200.

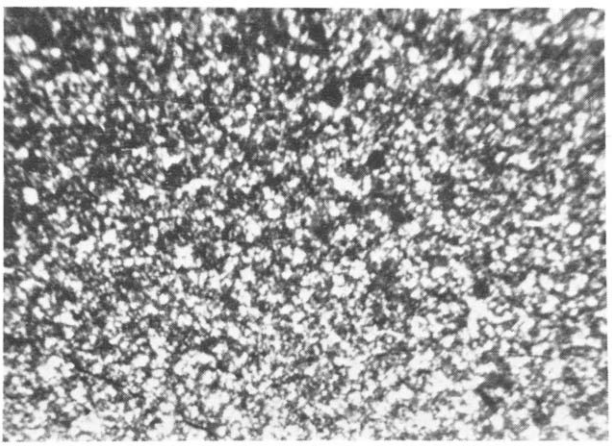

Fig. 21. Photomicrograph of G9-5.0% TiO_2 +0.4% ZrO_2 + 1% F; 630°C/4 h+780°C/1/2 h. Similar to Fig. 20, but slightly coarser. Crossed nicols, ×200.

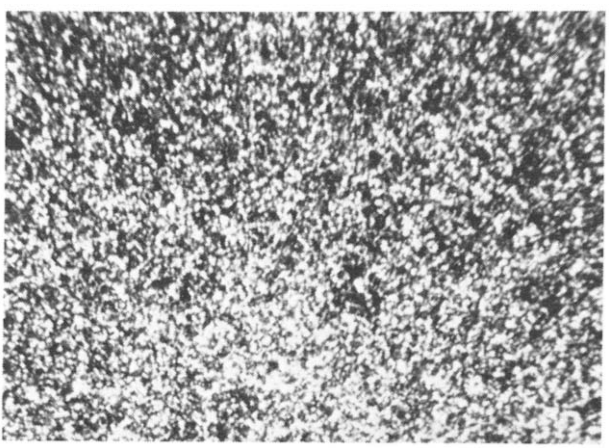

Fig. 22. Photomicrograph of G9-5.0% TiO_2 +0.4% ZrO_2; 660°C/4 h+780°C/1 h. Similar to Fig. 20, but of denser and finer texture. Crossed nicols, ×200.

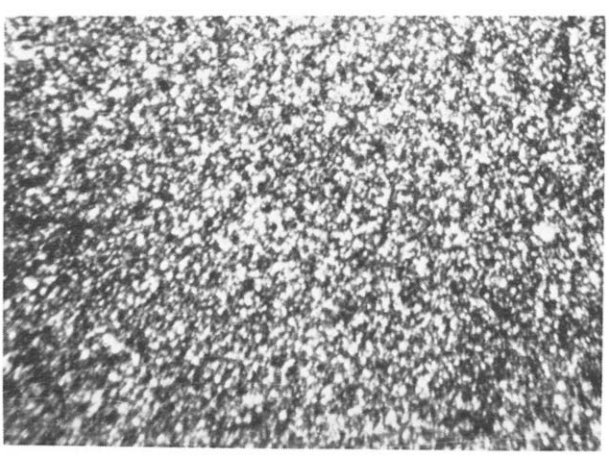

Fig. 23. Photomicrograph of G9-7.5% TiO_2; 660°C/4 h+780°C/1 h. Dense holocrystalline mass of uniform fine-grained texture. Crossed nicols, ×200.

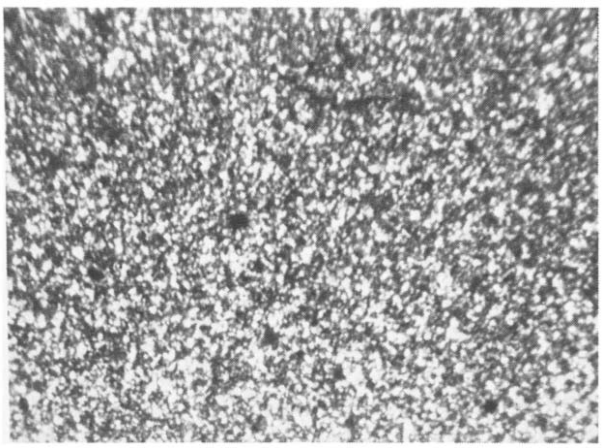

Fig. 24. Photomicrograph of G9-7.5% TiO_2 + 0.4% ZrO_2; 660°C/4 h + 780/1 h. Similar to Fig. 23. Crossed nicols, ×200.

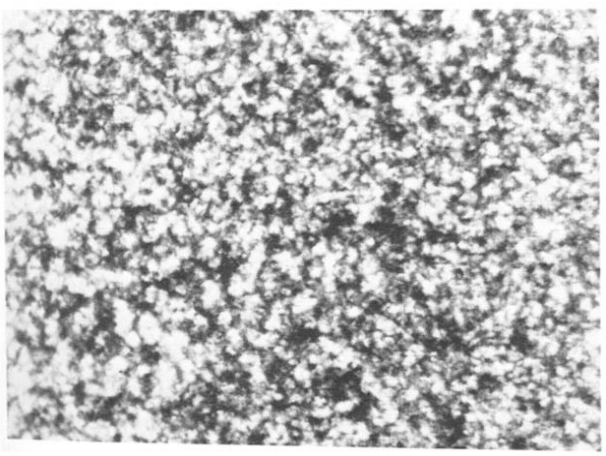

Fig. 25. Photomicrograph of G9-7.5% TiO_2 + 0.4% ZrO_2; 660°C/4 h + 900°C/1 h. Similar to Fig. 24, but of slightly coarser texture. Crossed nicols, ×200.

It is noteworthy that the formation and growth of the dendritic aggregates of G9-7.5t and G9-7.5t + 0.4z were always accompanied by a diffused interconnected pale brownish irregularly shaped glassy phase preferably distributed along the grain boundaries.

DISCUSSION

From the above results, it is quite evident that TiO_2 alone or with ZrO_2 or ZrO_2 + F is greatly effective in the nucleation and crystallization of the

studied glasses. Exceptions are compositions with high diopside contents (26.6 calculated mole %); namely G5, G7, G10 and G3 wherein such nucleators were less effective.

The incorporation of titania or titania mixtures in the base composition modified the crystallization kinetics, as expressed by the variations apparent in the peak temperatures and spans of the crystallization exotherms (e.g. Fig. 4). The nucleants also influenced the type of resulting crystalline phases, the transformation temperatures, the degree of metastability of β-Zn_2SiO_4 and β-eucryptite ss, and the texture of the resultant glass-ceramics. The introduction of TiO_2 or TiO_2 mixtures also showed a marked lowering in the temperature at which crystallization begins and, consequently, a widening of the crystallization range. This effect was increased with the increase in the nucleant concentration and also a synergistic effect was detected when 1% F was admixed with the $TiO_2 + ZrO_2$ mixture. This latter effect may be related to a change in glass viscosity, since additions of TiO_2 and F to glass are known to reduce its viscosity [1,27,28] and, consequently, lead to more mobilization of the glass-forming elements.

As regards the effect on the resulting crystalline phases, we find that the β-Zn_2SiO_4 phase was developed with some ease in the titania-free glasses (e.g., G9). By the addition of 2.5% TiO_2, almost no β-Zn_2SiO_4 was identified. This may be due to a catalytic effect of titania on the $\beta \rightarrow \alpha$(β-Zn_2SiO_4 $\rightarrow$ willemite) transformation. In willemite-rich base compositions, TiO_2 plays a great role in catalyzing the $\beta \rightarrow \alpha$ transition of zinc orthosilicates, or the direct crystallization of the α phase (willemite) in the resultant glass-ceramics (Table 2). Moreover, concentrations more than 2.5% TiO_2 showed a complete inhibition of any zinc silicate phase up to concentrations a little below 23 calculated mole % willemite in the base glass composition. This limit increases with the increase in the nucleant concentration and/or the decrease of heat-treatment temperature [e.g. Fig. 2(b)–(d)].

The addition of as low a concentration as 0.4% ZrO_2 to the TiO_2, especially to higher TiO_2 contents, showed rather more inhibition of willemite formation even at high temperatures. The retarding effect on willemite formation is interpreted herein as due to either or both of two mechanisms. Firstly, some of the Zn^{2+} intended to form willemite may have been accommodated in the diopside structure, aided by the presence of Ti^{4+} ions. This is evidenced by the change in the position and intensity of the X-ray diffraction lines of diopside [Figs. 2(g) and 3(f)]. Secondly, the TiO_2 may have reacted with ZnO to form a titanate phase (Zn_2TiO_4). This phase was also identified by X-ray particularly at higher concentrations of TiO_2 [Figs. 2(d) and (g) and 3(c)and (f)].

Fluorine ions, when included with $TiO_2 + ZrO_2$ showed the reverse effect. Samples nucleated with 5% $TiO_2 + 0.4\%$ $ZrO_2 + 1\%$ F showed a more

diagnostic development of willemite, even in the base glasses with lower calculated willemite concentrations or at lower heat-treatment temperatures [compare patterns (a) with (f) in Fig. 2]. This may be due to the powerful effect of fluorine ions in reducing the viscosity of the glass, and hence increasing the mobility of ions, thus facilitating willemite formation.

The effect of TiO_2 and TiO_2 mixtures on diopside formation was found to be contradictory to that on willemite formation. Though diopside was not crystallized in the titania-free glasses of G2, G4, G6 and G8, it was encountered in considerable amounts when these glasses were titania-nucleated (Table 2). Obviously, by titania nucleation of other base compositions a distinct increase in the crystallizing pyroxene phase was observed. The pyroxene resulting in these cases is actually a diopsidic ss (titanaugite) and its frequency increased with the increase of TiO_2 concentration in the base composition (cf. 2.99 and 2.53 Å lines in Figs. 2(a)–(d) and 3(a)–(c)]. On the other hand, the pyroxene developed in slowly cooled titania mixture-nucleated melt was proper diopsidic in composition. Yagi and Onuma [25] showed that $CaTiAl_2O_6$ can be soluble in diopside ($CaMgSi_2O_6$) at least up to 11% (4 wt. % TiO_2) and assumed that Ti^{4+} occupied octahedral positions and Al^{3+} tetrahedral positions; i.e. Mg^{2+} in $CaMgSi_2O_6$ is replaced by Ti^{4+} accompanied by the substitution of Si^{4+} by Al^{3+}. This may lead to an impoverishment, in our case, of the lithia-bearing minerals in Al^{3+} which, in turn, causes the appearance of silica-rich β-eucryptite and β-spodumene ss phases. Extensive solid solutions between silica and β-eucryptite or β-spodumene are well known [29–30]. Also, appreciable amounts of Mg^{2+} and Zn^{2+} can also be accommodated in both structures [4,17]. This, coupled with the Ti, Al for Mg, Si replacement, may explain the inhibition of willemite and development of titanaugite among the crystallization products. However, it seems probable that the Ti^{4+} accommodation in pyroxene varies according to the conditions of crystallization; mainly the degree of equilibria of the mineral-forming process.

TiO_2 nucleation up to a concentration of 5% did not affect the formation of the lithia minerals, where the resulting β-eucryptite ss and/or β-spodumene ss phases were more or less matching those developed in the original glass. The addition of 7.5% TiO_2 showed the siliceous character of these minerals, especially the β-spodumene ss, as well as giving a slight increase in the zinc titanate phase. The addition of 0.4% ZrO_2 to 7.5% TiO_2 corroborated this action showing a more siliceous character for the lithia minerals [Figs. 2(d), (g) and 3(c), (f)].

Regarding the β-eucryptite ss $\rightarrow$ β-spodumene ss transformation, TiO_2 had a catalytic effect on this transformation which increases with the increase in the titania content, and is markedly increased on the addition of 1% F. On the other hand, the addition of 0.4% ZrO_2 to TiO_2 showed a retarding effect

on this transformation; the transformation was slightly shifted to higher temperature values or, in other words, the stability field of β-eucryptite ss was widened. These effects are in agreement with those of Sack and Scheidler [19] who reported a stabilization of the high quartz ss phase in a Li_2O–MgO–Al_2O_3–SiO_2 glass nucleated by 2.5 wt. % TiO_2 and 2.5% ZrO_2. This result, along with other data [17–23] showed that TiO_2 preferentially nucleates in the keatite structure and ZrO_2 preferentially nucleates in the high quartz structure. However, the amounts of zirconia which they used were much higher than those tried in the present study and, consequently, no complete stabilization of the β-eucryptite ss structure was obtained over 900°C.

As for the nucleation effects on the textures of the resultant glass-ceramics, it was noted that if the TiO_2 concentration was reduced to 2.5% or below, the crystallization proceeded mainly by both surface and internal nucleations giving rise to non-uniform course-grained textures; while at 5% TiO_2 or above as well as mixtures of these and 0.4% ZrO_2 (or with additional 1% F) the crystallization took place by the internal nucleation mechanism giving rise to fine-grained uniform textures, i.e. satisfactory nucleation densities. It is also noteworthy that titania (or their mixtures) changed the growth habit of the crystallizing β-eucryptite ss phases from feathery or spherulitic textures (e.g. Fig. 5) to biconical or hedritic growths (e.g. Figs. 17 and 18). Barry and Lay [11] were able to attribute this to the inhibiting effect of Ti^{4+} on the growth rates of the β-quartz ss phase.

The promotion of fine-grain crystallization by TiO_2 has been ascribed to three basic mechanisms [1]. (i) A crystalline titania-rich phase, soluble in the melt and highly supersaturated in the glass, precipitates and heterogeneously nucleates the major phase. (ii) The same process occurs but it is preceded by glass-in-glass separation. (iii) TiO_2 lowers the surface energy for nucleation of solid phases [11].

In the present study, the clear scanning electron micrographs strongly support liquid–liquid phase separation on reheating the glass in the nucleation range. The observed phase separation is necessarily relevant to the subsequent nucleation; however we have no direct evidence of the link between them. One possibility is that phase separation causes crystallization of a titania-rich phase which nucleates the growth of β-quartz ss [8]. Another possibility is that the break up of the continuous network structure gives a high statistical probability that small short range regions of the β-quartz ss composition, being disconnected from neighbouring entanglement, will be converted to the crystalline state [12].

The more likely explanation of the action of TiO_2 and its mixtures on the nucleation process seems to enhance glass-in-glass phase separation, followed by the separation of a zinc titanate ss spinellide phase. This phase is

not, however, entirely confirmed by X-ray diffraction, especially with TiO_2 percentages lower than 7.5%, because its lines were overshadowed by the immediately formed β-eucryptite ss and titanaugite phases or may be due to its presence in amounts below the sensitivity of the X-ray diffractometer and/or its immature nature. In glasses containing 0.4% ZrO_2 in addition to TiO_2, the Zn_2TiO_4 ss phase was relatively more noticeable. So, although ZrO_2 is included to a very small extent in the nucleation mixture, its main role seems to enhance the ability of nuclei formation. On heating to slightly higher temperatures, this zinc titanate ss phase is then effective as a heterogeneous nucleating catalyst for the crystallization of β-eucryptite ss and titanaugite. A minor titania-rich phase developed during the amorphous phase separation was established by Barry et al. [13] using ESR spectra in lithia aluminosilicate glasses. This with other data [10,15] may corroborate the probability of the formation of a titania-rich crystalline phase after amorphous phase separation.

SUMMARY AND CONCLUSIONS

At the nucleant level studied, TiO_2, alone or mixed with other nucleators (ZrO_2 or $ZrO_2 + F$), was proved to be very effective on most of the compositions studied; especially the spodumene- and willemite-rich ones. TiO_2 additions lowered the onset crystallization temperature and favoured the crystallizability. They also catalyzed the transformation of the β-Zn_2SiO_4 and β-eucryptite ss formed initially into their stable forms and modified the crystallization products, especially by the inhibition of willemite-, and enhancement of pyroxene-formation in which process titanaugites are produced, their amounts being proportional to the TiO_2 content.

Addition of 0.4% ZrO_2 to TiO_2 showed a greater effect on both the enhancement of pyroxene formation and the inhibition of willemite formation, even at high temperatures, but oddly retarded the β-eucryptite ss $\rightarrow$ β-spodumene ss transformation. Addition of 1% F to the $TiO_2 + ZrO_2$ mixture showed a synergistic effect to the action of TiO_2, but greatly facilitated willemite formation.

The percent of titania accommodation in pyroxene varies according to the conditions of crystallization; mainly the degree of equilibria of the mineral-forming process. Besides, the formation of titanaugite from the glassy state, instead of proper diopside developed in a slowly cooled melt, is also undoubtedly influenced by the liquid phase separation (taking place on reheating the glass) possibly by an enrichment of one of the liquid phases by titania. These may also explain the difference in crystallization behaviour in the glass as compared with that in the molten state.

5 wt. % TiO_2 was found quite sufficient for internal nucleation. Uniform fine-grained textures were easily obtained therefrom. The most nucleation was obtained, however, by 5% TiO_2 + 0.4% ZrO_2 additions. The action of TiO_2 or its mixtures on the nucleation process seems to be the enhancement of liquid–liquid phase separation on reheating the glass followed by the separation of a zinc titanate phase which acts as a heterogeneous nucleating center for subsequent crystallization.

REFERENCES

1 P.W. McMillan, Glass-Ceramics, Academic Press, London, 2nd edn., 1979.
2 D.R. Stewart, in L.D. Pye, H.J. Stevens and W.C. LaCourse (Eds.), Introduction To Glass Science, Plenum, New York, 1973, pp. 237–271.
3 E.A. Porai-Koshits, in N.A. Toropov and E.A. Porai-Koshits, (Eds.), The Structure of Glass, Vol. 5, Consultants Bureau, New York, 1965, pp. 1–8.
4 G.H. Beall and D.A. Duke, in R. Uhlmann and N.J. Kreidl (Eds.), Treatise on Glass Science and Technology, Preprint, Academic Press, New York, 1980.
5 S.D. Stookey, Ind. Eng. Chem., 51 (1959) 805.
6 S.D. Stookey, U.S. Pat. 2,920,971, 1960.
7 A.W.A. El-Shennawi, Ph.D. Thesis, Cairo University, Cairo, Egypt, 1978.
8 W. Hinz and P.O. Kunth, Silikat Tech., 11 (1960) 506.
9 R.D. Maurer, J. Appl. Phys., 33 (1962) 2132.
10 P.E. Doherty, D.W. Lee and R.S. Davis, J. Am. Ceram. Soc., 50 (2) (1967) 77.
11 T.I. Barry and L.A. Lay, in J.W. Mitchell, R.C. De Vries, R.W. Roberts and P. Cannon (Eds.), Reactivity of Solids, Wiley, New York, 1969, pp. 685–694.
12 T.I. Barry, D. Clinton, L.A. Lay, R.A. Mercer and R.P. Miller, J. Mater. Sci., 4 (1969) 596; 5 (1970) 117.
13 T.I. Barry, L.A. Lay and R.P. Miller, Discuss. Faraday Soc., 50 (1970) 214.
14 M. Tashiro and M. Wada, Advances in Glass Technology, Plenum Press, New York, 1963, Part 2, pp. 18–19.
15 G.F. Neilson, in L.L. Hench and S.W. Freiman (Eds.), Advances in Nucleation and Crystallization in Glasses, Am. Ceram. Soc. Spec. Publ., No. 5, 1972, pp. 73–82.
16 A. Ali, Trans. Indian Ceram. Soc., 27 (4) (1968) 140.
17 G.H. Beall, B.R. Karstetter and H.L. Rittler, J. Am. Ceram. Soc., 50 (4) (1967) 181.
18 G.H. Beall and D.A. Duke, J. Mater. Sci., 4 (1969) 340.
19 W. Sack and H. Scheidler, Glastech. Ber., 39 (3) (1966) 126.
20 W.E. Smith, U.S. Pat. 3,380,818, 1968.
21 Y. Moriya, J. Ceram. Assoc. Jpn., 76 (1968) 293.
22 D.R. Stewart, in L.L. Hench and S.W. Freiman (Eds.), Advances in Nucleation and Crystallization in Glasses, Am. Ceram. Soc. Spec. Publ., Vol. 5, 1972, pp. 83–90.
23 H. Scheidler and W. Sack, Proc. 9th Int. Congr. Glass, Paris, 1971, pp. 1069–1085.
24 W.A. Deer, R.A. Howie and J. Zussman, Rock-Forming Minerals, Vol. 2, Longmans, London, 1963.
25 K. Yagi and K. Onuma, J. Fac. Sci. Hokkaido Univ. Ser. IV, 13 (1967) 463.
26 Inorganic Index to the Powder File. A.S.T.M. Publications PDIS, 1968.
27 W.A. Weyl, Coloured Glasses, Society of Glass Technology, Sheffield, 1959.

28 A.G.F. Dingwall and H. Moore, J. Soc. Glass Technol., 37 (1953) 316.
29 R. Roy, J. Am. Ceram. Soc., 43 (12) (1960) 670.
29 R. Roy, Z. Kristallogr., 111 (3) (1959) 185.
30 W. Ostertag, G.R. Fischer and J.P. Williams, J. Am. Ceram. Soc., 51 (11) (1968) 651.